JOURNAL OF SOLID STATE CHEMISTRY 88, 163–176 (1990)

123, 247, and 124 Cuprate Superconductors: Investigations of Thermodynamic Stabilities, Defect Structures, and Intergrowths[1]

C. N. R. RAO[2] G. N. SUBBANNA, R. NAGARAJAN, A. K. GANGULI, L. GANAPATHI, R. VIJAYARAGHAVAN, S. V. BHAT, AND A. R. RAJU

Indian Institute of Science, Bangalore 560012, India

Received April 18, 1990

DEDICATED TO J. M. HONIG ON THE OCCASION OF HIS 65TH BIRTHDAY

Careful investigations employing nonresonant microwave or rf absorption, Cu^{2+} EPR spectra, X-ray diffraction, and electron microscopy show that orthorhombic $YBa_2Cu_3O_{7-\delta}$ is thermodynamically stable and monophasic when δ is 0.0–0.2 (T_c = 90 K), 0.25 (T_c = 80 K), and 0.5 (T_c = 45 K). The last two compositions are associated with ordered oxygen-vacancy structures; in the δ = 0.0–0.2 regime, $3b = c$. Compositions in the range δ = 0.3–0.4 (T_c = 60 K) do not appear to be thermodynamically stable and decompose on annealing, suggesting thereby that the so-called 60 K superconducting phase in the $YBa_2Cu_3O_{7-\delta}$ system may not be genuine. 123 cuprates prepared with excess CuO often show fringes of 124 in lattice images. Both 124 and 247 cuprates prepared by the ceramic method in a flowing oxygen atmosphere frequently show intergrowths of each other or with 123. Such epitaxial relationships between 123, 124, and 247 cuprates could be of significance with respect to their superconducting properties. Both 124 and 247 cuprates undergo thermal decomposition to give 123 and CuO.

Introduction

Superconducting $YBa_2Cu_3O_{7-\delta}$ is orthorhombic over the δ range 0.0–0.6 and exhibits a T_c of around 90 K when $0.0 \lesssim \delta \lesssim 0.2$. The T_c shows a second plateau at 60 K over the composition range $0.25 < \delta \lesssim 0.4$ (*1*). In spite of the exhaustive studies carried out on the $YBa_2Cu_3O_{7-\delta}$ system in the last 3 years, there is still considerable uncertainty regarding the monophasic nature as well as the thermodynamic stability at different oxygen stoichiometries. The two T_c regimes have been associated with differently related orthorhombic lattice parameters (*2*), but Beyers *et al.* (*3*) suggest that $YBa_2Cu_3O_{7-\delta}$ may not be truly monophasic both in the 90 K ($0.0 \lesssim \delta \lesssim 0.2$) and the 60 K ($0.25 < \delta \lesssim 0.4$) regimes. According to Beyers *et al.* (*3*), the cuprate is monophasic only around $\delta \approx 0.25$ where there is a sharp change in T_c with δ as evidenced in the $T_c - \delta$ phase diagram. We were interested in examining whether indeed this is true, having had some doubts with regard to the monophasic nature of the compositions in the 60 K T_c regime based on some of our recent observations.

[1] Contribution No. 698 from the Solid State and Structural Chemistry Unit dedicated to Professor J. M. Honig, a dear friend of one of us (C.N.R.R.), for over 3 decades.

[2] To whom correspondence should be addressed.

0022-4596/90 $3.00

It has been suggested that some of the $YBa_2Cu_3O_{7-\delta}$ compositions may be inherently unstable toward decomposition into orthorhombic and tetragonal phases (*4, 5*). If so, it is of interest to find out in which stoichiometry range such a decomposition occurs and to investigate the process by which the decomposition occurs. We have attempted to answer some of these questions in the present study by a combined use of X-ray diffraction, high-resolution electron microscopy, electrical and magnetic measurements, nonresonant microwave absorption, and EPR spectroscopy. It is to be noted that nonresonant microwave absorption can be used as a means of detection of superconductivity (*6*), while the Cu^{2+} resonance in the EPR spectra is a useful diagnostic tool to characterize oxygen-deficient cuprate phases.

In addition to the study of the $YBa_2Cu_3O_{7-\delta}$ system, we have carried out the synthesis and characterization of a few 124 cuprates of the formula $LnBa_2Cu_4O_8$ (*Ln* = Y or rare earth) containing two Cu–O chains and also of 247 cuprates of the formula $Ln_2Ba_4Cu_7O_{15}$ involving an intergrowth of alternate units of 123 and 124 cuprates. We have employed the ceramic method for the synthesis of the 124 and 247 compounds in flowing oxygen at 1 atm instead of the use of high oxygen pressures (*7–10*). Of special interest to us was the facility with which the 123, 124, and 247 cuprates can intergrow, a feature that could be relevant to the use of these materials for technological applications. Both 124 and 247 cuprates decompose to 123 and CuO on heating and the 123 cuprate so obtained could be different from the prepared directly in terms of micro and ultramicro structures.

Experimental

Samples of $YBa_2Cu_3O_{7-\delta}$ were prepared by heating stoichiometric quantities of Y_2O_3, BaO_2, and CuO around 1240 K for 24 hr. Samples with different δ values are obtained by varying the heat treatment and/or annealing in a O_2/N_2 atmosphere. Iodometric titrations were carried out to determine the oxygen stoichiometry of these samples. Decomposition of $YBa_2Cu_3O_{7-\delta}$ was carried out in dry air at 470 K for 50–100 hr.

Samples of $LnBa_2Cu_4O_8$ (*Ln* = Gd, Dy, Ho, and Y) were prepared by heating a mixture of stoichiometric quantities of Ln_2O_3, $Ba(NO_3)_2$, and CuO with up to 20 mol% of $NaNO_3$ or Na_2O_2 at 973 K for 30 min followed by grinding, pelletizing, and heating in flowing oxygen at 1073 K for a minimum period of 24 hr (*9, 10*). The monophasic nature of the samples improves with repeated grinding and heating. Samples of $Ln_2Ba_4Cu_7O_{15}$ (*Ln* = Gd, Dy, and Y) were synthesized by a procedure similar to that employed for 124, but for the difference in the sintering temperature. Nearly monophasic samples of 247 are obtained by sintering around 1133 K for a minimum period of 24 hr. Thermal decomposition of 124 and 247 compounds to 123 compounds was carried out in oxygen at 1193 K for 3 hr.

X-ray powder diffraction patterns of the cuprates were recorded with a JEOL JDX-8P diffractometer using Cu$K\alpha$ radiation. Electron microscopy was carried out using a JEOL JEM-200CX electron microscope operating at 200 kV. Fourprobe dc resistivity and dc magnetic susceptibility measurements were carried out to characterize the superconducting properties. Nonresonant microwave absorption as well as Cu^{2+} EPR measurements were carried out with a Varian ESR spectrometer (9.1 GHz). The experiments in the rf range were carried out using a conventional CW NMR spectrometer with a level-limited Robinson-type oscillator serving as the rf source [nominal frequency, 17 MHz]; frequencies were measured using a Hewlett–Packard frequency counter, temperature regulation and variation was achieved with an Oxford In-

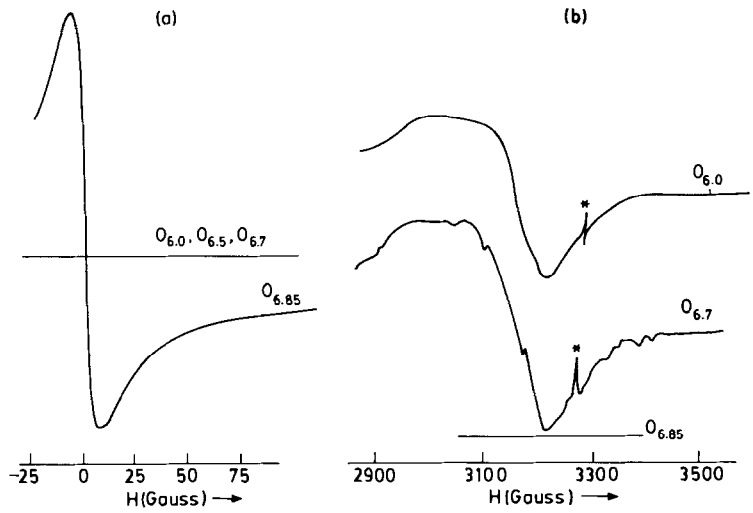

FIG. 1. (a) Nonresonant microwave absorption of $YBa_2Cu_3O_{7-\delta}$ (δ = 0.15, 0.3, 0.5, and 1.0) at 77 K; (b) Cu^{2+} EPR signal of $YBa_2Cu_3O_{7-\delta}$ (δ = 0.15, 0.3, and 1.0) at 300 K. Asterisk indicates signal due to DPPH.

struments continuous flow cryostat. The absorption signals were recorded after field modulation at ~67 Hz and lock-in detection.

Results and Discussion

The $YBa_2Cu_3O_{7-\delta}$ System

We shall first summarize the results from nonresonant microwave absorption and EPR measurements on different compositions of the $YBa_2Cu_3O_{7-\delta}$ system along with the information on the defect structures:

(a) Superconducting $YBa_2Cu_3O_{7-\delta}$ compositions in the δ range of $0.0 < \delta \lesssim 0.2$ ($T_c \sim 90$ K) show nonresonant microwave absorption at and below 90 K (Fig. 1). They do not show Cu^{2+} resonance in the EPR spectra. The EPR-silence can be taken to indicate the absence of localized moment on Cu and also the absence of a highly oxygen-deficient composition as an impurity or as a component in a possible mixture. There is no definitive evidence from electron diffraction for defect ordering in this stoichiometry range, especially close to $\delta = 0.0$, but the orthorhombic c-parameter is exactly equal to $3b$ over this entire range of compositions as shown in Fig. 2.

(b) $YBa_2Cu_3O_{7-\delta}$ compositions with δ = 0.3–0.4 ($T_c \sim 60$ K) do not show nonresonant microwave absorption at 77 K (Fig. 1). Since we could not study nonresonant microwave absorption below 77 K, we ex-

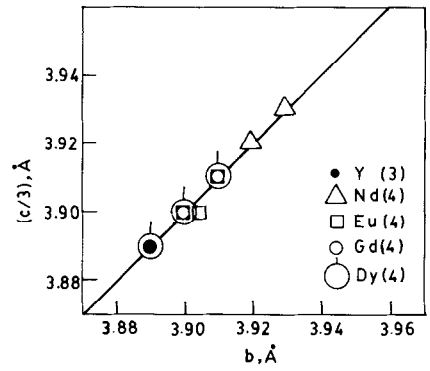

FIG. 2. Plot of b versus $c/3$ of $LnBa_2Cu_3O_{7-\delta}$ in the 90 K T_c region. Experimental points and the $c = 3b$ theoretical line are both shown. Notice how close the experimental points fall on the theoretical line.

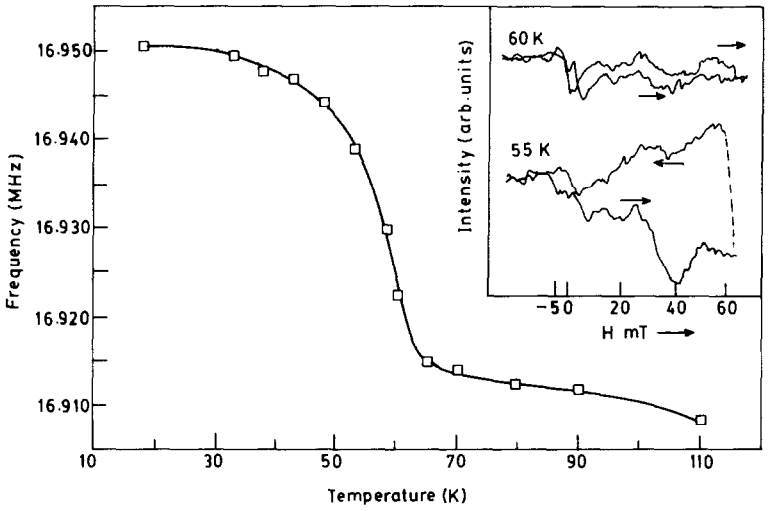

FIG. 3. Variation of resonance frequency of the rf oscillator as a function of temperature for the $YBa_2Cu_3O_{6.7}$ compound. Inset shows rf absorption signals at two different temperatures.

amined $YBa_2Cu_3O_{6.7}$ ($T_c \sim 60$ K) in the rf range using a conventional CW NMR spectrometer. We had shown earlier (*6*) that such experiments provide information similar to that obtained by microwave absorption measurements. In Fig. 3 we show the frequency of the oscillator (in whose tank coil, the sample is kept) as a function of temperature. We notice a slow increase in the frequency down to ~60 K at which temperature there is a marked increase. This frequency change is a sensitive indicator of the superconducting transition. Although the rf absorption signal appears to be very weak, the frequency change can be measured easily to characterize the superconducting transition. In the inset of Fig. 3, we show the rf absorption signal at two temperatures. The signal is not only weak and noisy but also complex possibly due to the nature of the cuprate phase at this oxygen stoichiometry. Well-annealed preparations in the rane $\delta = 0.3$–0.4 show a weak Cu^{2+} resonance in the EPR spectrum (Fig. 1). Quenched preparations, however, show moderate to intense Cu^{2+} EPR signals.

(c) $YBa_2Cu_3O_{6.75}$ is distinctly different from the compositions in the range $\delta = 0.3$–0.4 (*5*); the former shows a T_c close to 80 K and has a well-defined defect structure with a unit cell of $2\sqrt{2}a_c \times 2\sqrt{2}a_c = 3a_c$ as shown in Fig. 4. The $0_{6.75}$ composition exhib-

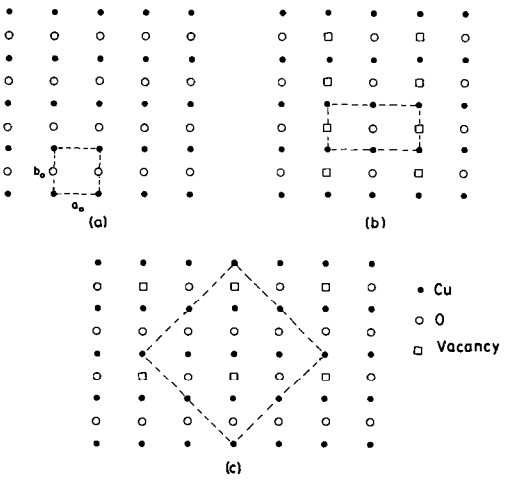

FIG. 4. Structure of the basal plane of the unit cell of $YBa_2Cu_3O_{7-\delta}$: (a) $\delta = 0.0$, (b) $\delta = 0.5$, and (c) $\delta = 0.25$.

its nonresonant microwave absorption at 77 K, but no Cu^{2+} EPR signal.

(d) $YBa_2Cu_3O_{6.5}$ has alternate chains with fully occupied (O_7 type) and vacant (O_6 type) O1 sites along the *b*-axis (*5, 11*). It is to be underscored that $YBa_2Cu_3O_{6.5}$ with a T_c of ~45 K is not a mixture of $YBa_2Cu_3O_7$ and $YBa_2Cu_3O_6$; the mixture is likely to have exhibited a T_c of ~90 K. The interchain ordering doubles the periodicity of the *a*-axis as shown in Fig. 3 and the unit cell is $2a_c \times a_c \times 3a_c$. $YBa_2Cu_3O_{6.5}$ shows no nonresonant microwave absorption down to 50 K.

(e) $YBa_2Cu_3O_6$ being antiferromagnetic with a well-defined T_N (~450 K) shows a clear anisotropic Cu^{2+} EPR signal, but no nonresonant microwave absorption (Fig. 1). The intensity of the EPR signal increases with decrease in the temperature in the range 77 K–300 K where the material is antiferromagnetic.

The above results suggest that $YBa_2Cu_3O_{7-\delta}$ ($0.0 < \delta \lesssim 0.2$) with a characteristic T_c of 90 K is certainly a well-defined monophasic system with a moderate homogeneity range. Accordingly, $3b = c$ in this region, suggesting that the oxygen vacancies up to $\delta = 0.2$ are accommodated without affecting the superconductivity or the structural features. The composition $YBa_2Cu_3O_{6.5}$ with interchain ordering along the *b*-axis is also an ordered monophasic composition. $YBa_2Cu_3O_{6.75}$ with interchain ordering along the *b*-axis also appears to be an ordered, monophasic composition. The only difficulty lies with the range $0.25 < \delta \lesssim 0.40$ showing a T_c of ~60 K. Although many of the compositions in this range show some diffuse scattering or superlattice spots in the electron diffraction patterns, it seems likely that they are not truly thermodynamically stable. The features in diffraction patterns could arise from mixtures or more likely intergrowths of differently ordered oxygen-deficient phases. Accordingly, we almost always observe Cu^{2+} EPR signals in the compositions with $\delta = 0.3$–0.4. The observation of a constant T_c of 60 K is itself not difficult to understand. In this composition range, every addition of oxygen oxidizes a Cu^{1+} of the chain to Cu^{2+}, not affecting the hole concentration in the Cu–O sheets. The plateau at 60 K in the $T_c - \delta$ diagram may therefore be indicative of the constancy in the hole concentration in the Cu–O sheets in this composition range. What seems plausible is that the compositions in the δ range of 0.3 to 0.4 may be metastable arising from a rather disordered oxygen vacancy arrangement with a tendency to transform into more stable phases such as $YBa_2Cu_3O_{6.9}$ and $YBa_2Cu_3O_{6.5}$. We have indeed found evidence for such a transformation of $YBa_2Cu_3O_{6.7}$ on prolonged annealing as suspected by Hou *et al.* (*5*).

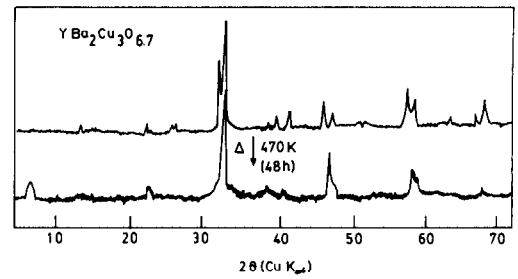

FIG. 5. Powder X-ray diffraction pattern of $YBa_2Cu_3O_{6.7}$ before and after annealing at 470 K for 50–100 hr.

On heating orthorhombic $YBa_2Cu_3O_{6.7}$ (T_c ~ 60 K) for 50 to 100 hr at 470 K in dry air, the X-ray diffraction pattern changes markedly (Fig. 5). We notice that the 200 and 020 reflections characteristic of the orthorhombic structure are not seen in the pattern of the sample subjected to the heat treatment. The X-ray diffraction pattern of the thermal-annealed sample resembles that of a tetragonal perovskite, but for the low-angle reflection ($d \sim 13.5$ Å). In the electron diffraction pattern, we find marked streaking along the *c*-axis in the product obtained after annealing at 470 K for 50–100 hr (Fig. 6a). This probably results from the absence

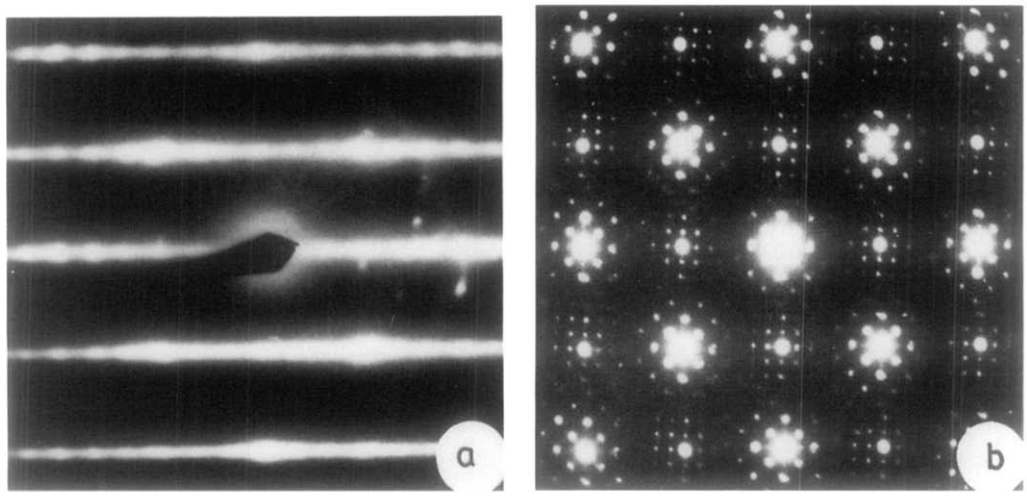

FIG. 6. (a) SAED pattern recorded along (100) direction of $YBa_2Cu_3O_{6.7}$ after annealing in air at 470 K for 50–100 hr showing extensive streaking along c-axis; (b) SAED pattern recorded along (001) direction of $YBa_2Cu_3O_{6.7}$ annealed in air at 470 K for 50–100 hr showing multiple diffraction.

of registry along the c-axis caused by the extensive oxygen disorder in the ab-plane (between the O1 and O5 positions). Accordingly, we see no twins in the bright field image of the product obtained after thermal treatment, while the starting $YBa_2Cu_3O_{6.7}$ shows extensive twins (Fig. 7). Electron diffraction patterns of some of the crystals of the annealed product show multiple diffraction phenomena due to misoriented areas (Fig. 6b). Such features in the diffraction patterns could arise from the superposition of disoriented lamallae.

Some of the crystals of the thermally treated product exhibit 13.5 Å fringes along the c-axis in the lattice image (Fig. 8). The 13.5 Å fringes closely correspond to $Y_2Ba_4Cu_7O_{15}$ (247) or $YBa_2Cu_4O_8$ (124) containing one and a half or two Cu–O chains, respectively. The low-angle reflection in the X-ray diffraction pattern ($d \sim 13.5$ Å) can also, in principle, be considered to be due to the 247 or the 124 phase. We do not, however, observe the main reflections of the 247 and 124 phases expected around d values of 2.74 and 2.72 Å in the X-ray diffraction patterns. A this stage, we only propose that a nearly tetragonal structure involving highly disordered chain oxygens is formed initially on heating $YBa_2Cu_3O_{6.7}$ for 50–100 hr at 470 K. This disordered phase is probably the precursor to the decomposition or disproportionation that occurs on heating $YBa_2Cu_3O_{6.7}$ for extended periods of 200 hr or more (*12*). X-ray diffraction patterns show the formation of a mixture of orthorhombic and tetragonal phases on such prolonged heating. The mixture has a T_c close to 90 K, although the starting composition itself has a T_c of 60 K. The T_c of 90 K results from an orthorhombic phase with δ in the range 0.0–0.2 while the tetragonal phase would be nonsuperconducting.

As expected, annealed samples of $YBa_2Cu_3O_{6.7}$ ($T_c \sim 60$ K), which do not show nonresonant microwave absorption at 77 K, show it on heating at 470 K for 50–100 hr or longer, indicating thereby the formation of a phase with higher T_c (probably $YBa_2Cu_3O_{6.9}$) as shown in Fig. 9. We also find that the Cu^{2+} EPR signal becomes more intense on heating. This is expected because

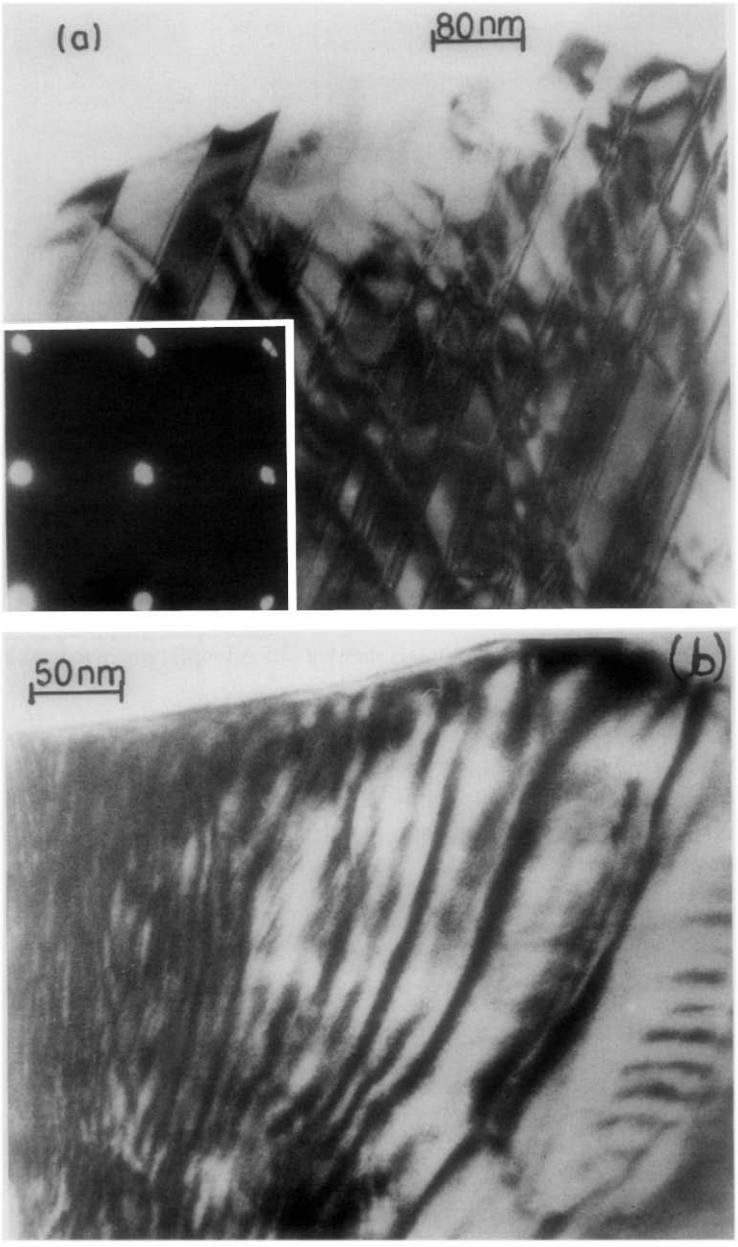

FIG. 7. (a) Bright-field image of twins in $YBa_2Cu_3O_{6.7}$ (inset shows that SAED pattern); (b) Bright-field image of $YBa_2Cu_3O_{6.7}$ after annealing at 470 K.

of the formation of the nonsuperconducting tetragonal phase with high δ.

Unlike $YBa_2Cu_3O_{6.7}$, heating $YBa_2Cu_3O_{6.85}$ or $YBa_2Cu_3O_{6.90}$ at 470 K for 100 hr does not result in any significant changes in the X-ray and electron diffraction patterns or in the other properties. It seems that decomposition is only exhibited by composi-

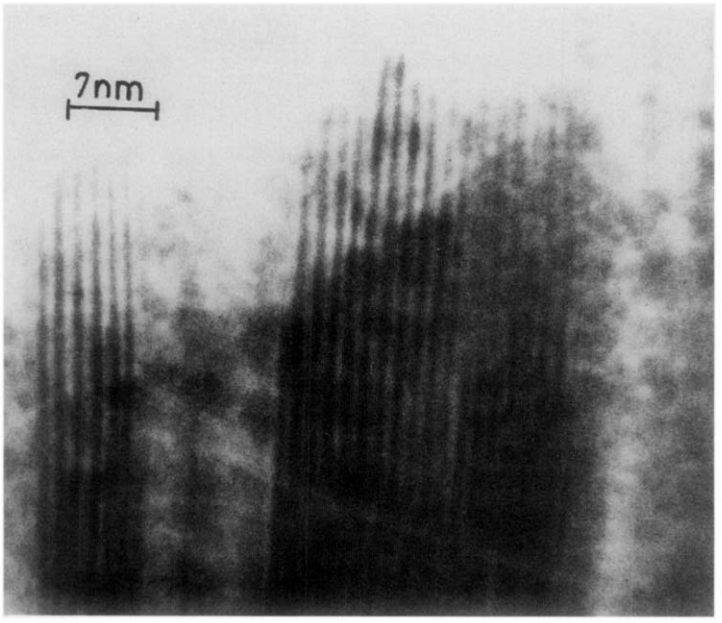

FIG. 8. Lattice image of annealed $YBa_2Cu_3O_{6.7}$ showing 13.5 Å fringes; amorphous regions can also be seen in the image.

tions close to $YBa_2Cu_3O_{6.7}$. This result reinforces our earlier conclusion that while $YBa_2Cu_3O_{6.9}$ is stable and monophasic, $YBa_2Cu_3O_{6.7}$ is thermodynamically metastable and probably composed of intergrowths (*13*, *14*) of differently ordered oxygen-va-

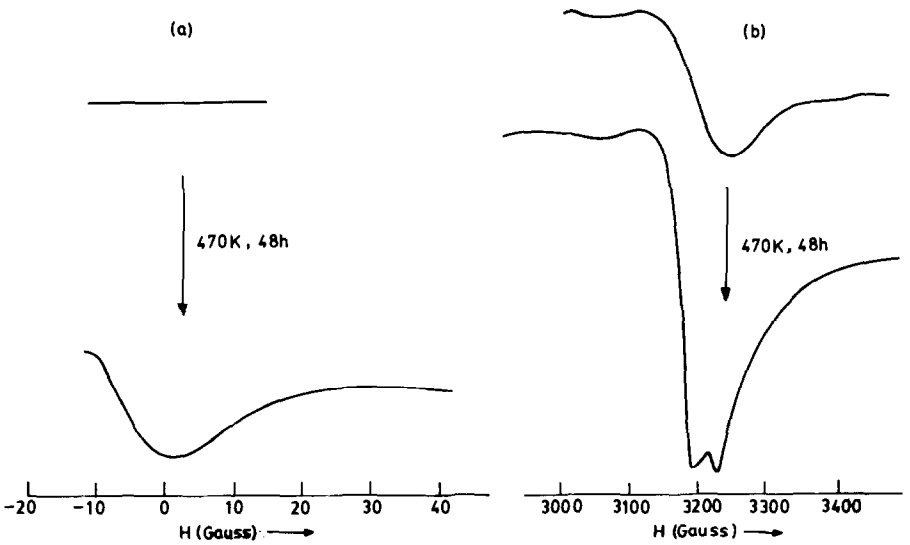

FIG. 9. (a) Nonresonant microwave absorption (at 77 K) of $YBa_2Cu_3O_{6.7}$ before and after annealing at 470 K for 50 hr; (b) Cu^{2+} EPR signal of $YBa_2Cu_3O_{6.7}$ before and after annealing at 470 K.

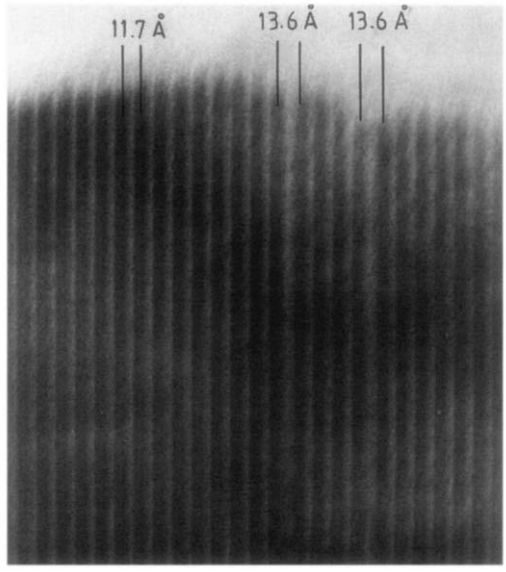

FIG. 10. Lattice image of $YbBa_2Cu_3O_7$ prepared with excess CuO; image shows the intergrowth of 124 (13.6 Å) in the matrix of 123 (11.7 Å).

cancy structures, and decomposing to more stable phases on annealing as suspected by Hou *et al.* (*5*).

124 and 247 cuprates

123 cuprates prepared with a starting mixture containing excess CuO can result in the formation of some 124 cuprate. Thus, $YbBa_2Cu_3O_7$ which can only be prepared with excess CuO (*15*) shows fringes due to 124 (13.6 Å) in the electron microscopic images (Fig. 10). In this section we shall discuss the characterization of 124 and 247 cuprates and intergrowth structures involving them by electron microscopy.

In Fig. 11 we show the X-ray diffraction patterns of a few of the 124 and 247 cuprates synthesized by us by the ceramic method in a flowing oxygen atmosphere. The unit cell dimensions of the 124 and 247 cuprates as determined from X-ray and electron diffraction studies are $a \simeq 3.84$, $b \simeq 3.87$, $c \simeq 27.23$ Å and $a \simeq 3.85$, $b = 3.87$, and $c = 50.29$ Å, respectively. In Fig. 12, we show a lattice image of $HoBa_2Cu_4O_8$ recorded along the (100) direction along with the selected area electron diffraction (SAED) pattern. We clearly see the 13.6 Å fringes corresponding to one-half of the *c*-parameter. In the same micrograph, we show a region (circled)

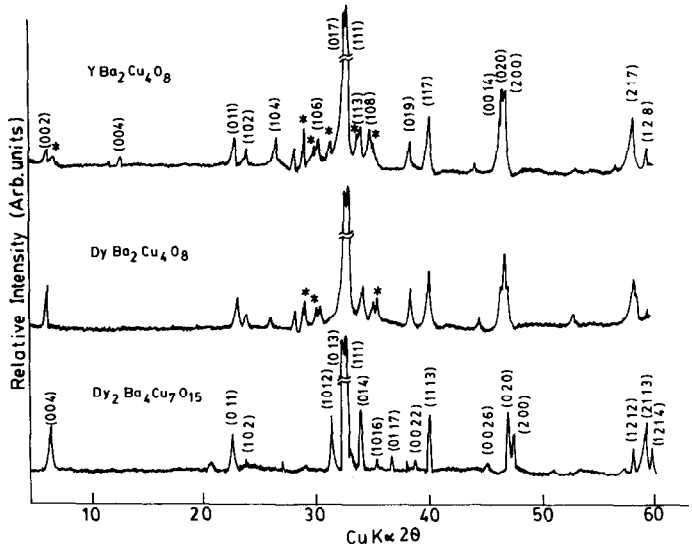

FIG. 11. X-ray powder diffraction patterns of a few of 124 and 247 cuprates. Asterisk indicates impurity reflections due to 123, $BaCuO_2$, CuO, etc.

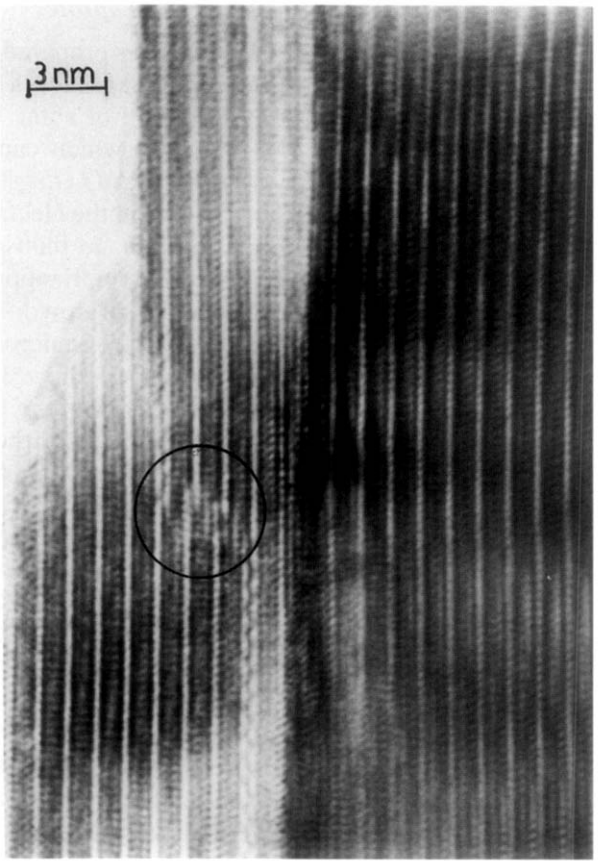

FIG. 12. High-resolution electron microscopic image of $HoBa_2Cu_4O_8$ in [100] orientation. Notice fringes of 13.6 Å corresponding to one-half of the *c*-parameter. Circled region shows displacement of Ho/Ba layers.

where there is a displacement of the Ho/Ba layers. High-resolution electron microscopic images of two 247 cuprates (Gd and Dy) are shown in Fig. 13. The corresponding SAED patterns are shown in the insets. The images show the expected 25 Å fringes equal to one-half of the *c*-parameter. Lattice images of the 247 compounds clearly show how they are a result of the recurrent intergrowth of 123 and 124 units. Some of the images of the 247 cuprates show the occasional presence of fringes due to 124 units. This is not surprising in view of the nearly identical *a*- and *b*-parameters of the 123, 124, and 247 cuprates and the consequent, natural "epitaxial" relationship among them. It should be noted that layered bismuth oxides possessing general formula $Bi_2A_{n-1}Bn_nO_{3n+3}$ extensively form intergrowth structures (*13, 14*). In Fig. 14, we show a high-resolution image of $DyBa_2Cu_4O_8$ with random intergrowth of 124 and 247 giving rise to 13.6 and 25 Å fringes, respectively. In Fig. 15 we show the electron micrograph of an intergrowth in $YBa_2Cu_4O_8$ where 11.7 and 25 Å fringes corresponding to 123 and 247 occur. The electron diffraction pattern also substantiates the presence of such an intergrowth. Accordingly, we see Bragg spots corresponding to 11.7 and 25 Å. Since

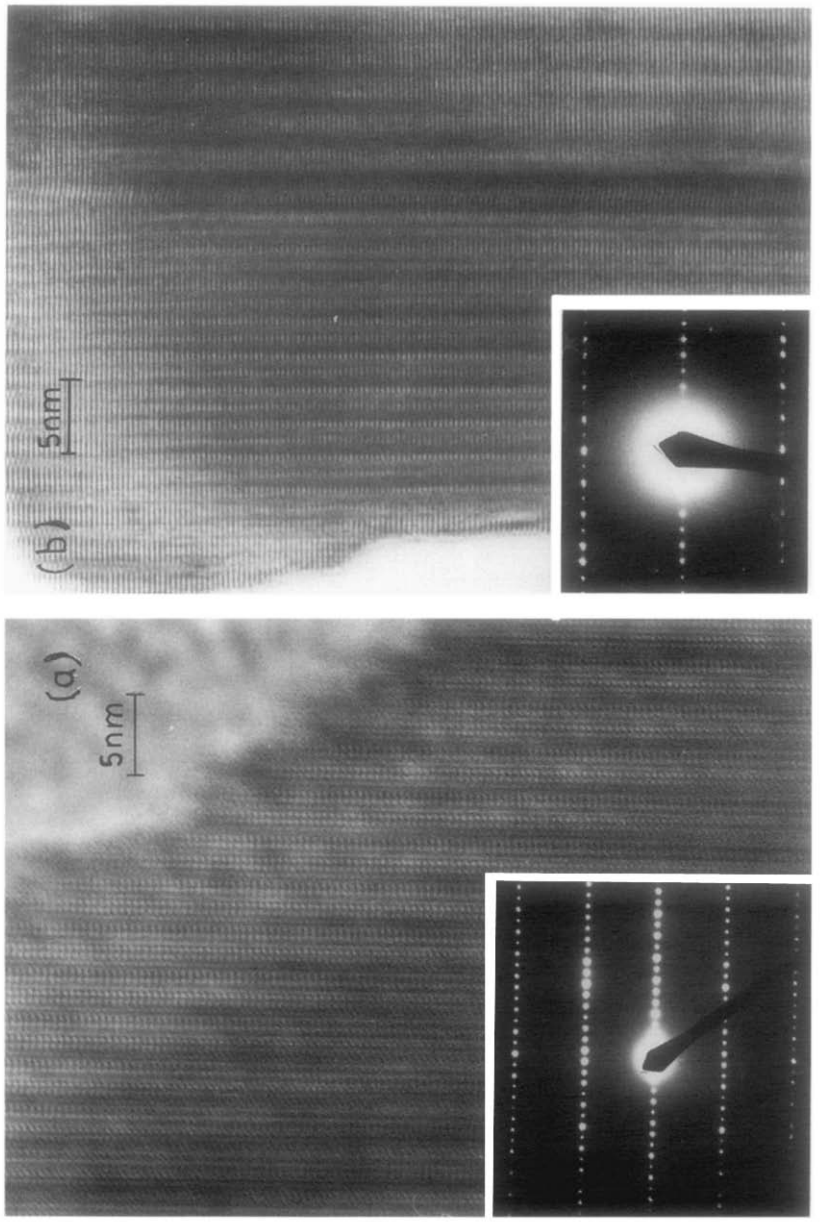

FIG. 13. (a) High-resolution electron microscopic $Dy_2Ba_4Cu_7O_{15}$ in [110] orientation. Inset shows the corresponding SAED pattern; (b) High-resolution electron microscopic image of $Gd_2Ba_4Cu_7O_{15}$ in [100] orientation. Inset shows the SAED pattern. Notice the 25 Å fringes corresponding to one-half of c-parameter.

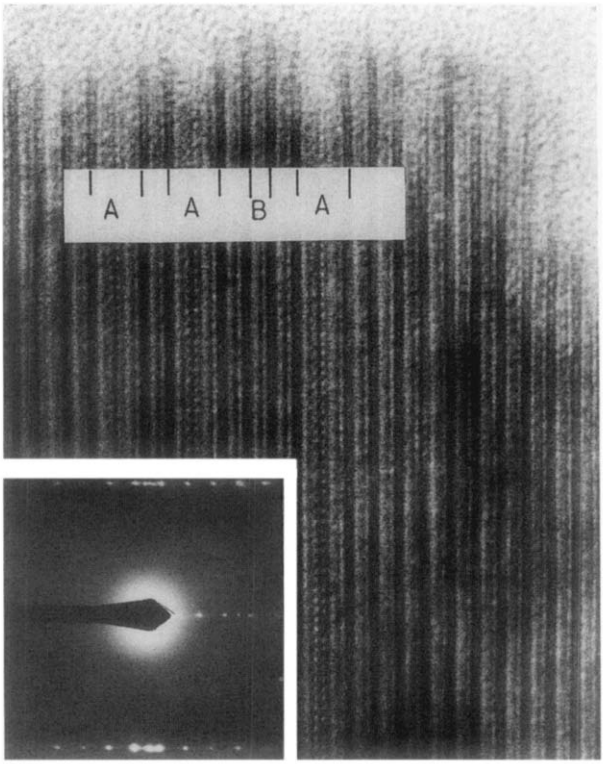

FIG. 14. High-resolution electron micrograph of $DyBa_2Cu_4O_8$ showing 25 Å (A) and 13.6 Å (B) fringes due to random intergrowth. Inset shows SAED pattern.

247 itself results from the recurrent intergrowth of 123 and 124, we could consider the features in Figs. 13 and 14 as due to the intergrowth of 123 and 124 units.

In many preparations of 247, we have noticed the formation of 123 crystals as confirmed from powder X-ray diffraction and electron microscopy. One of the characteristic features of the orthorhombic 123 cuprates is the formation of twins, absent in both 124 and 247 compounds. In the micrograph shown in Fig. 16, we see a microdomain structure as well as the twin structure of 123.

When 124 and 247 are heated at about 1193 K in oxygen for 5–12 hr, they decompose to give 123 throwing out excess CuO. This could be readily verified from both X-ray diffraction and electron microscopy.

The temperature variation of the normalized resistance of a few 124 and 247 cuprates are shown in Fig. 17. The onset of superconductivity in the 124 compounds is 80 K; the onset in the 247 compounds is around 70 K. DC magnetic susceptibility data shown in Fig. 17 also establish the superconducting nature of these samples. The 123 compound obtained by the thermal decomposition of 124 show the onset of superconductivity ~90 K.

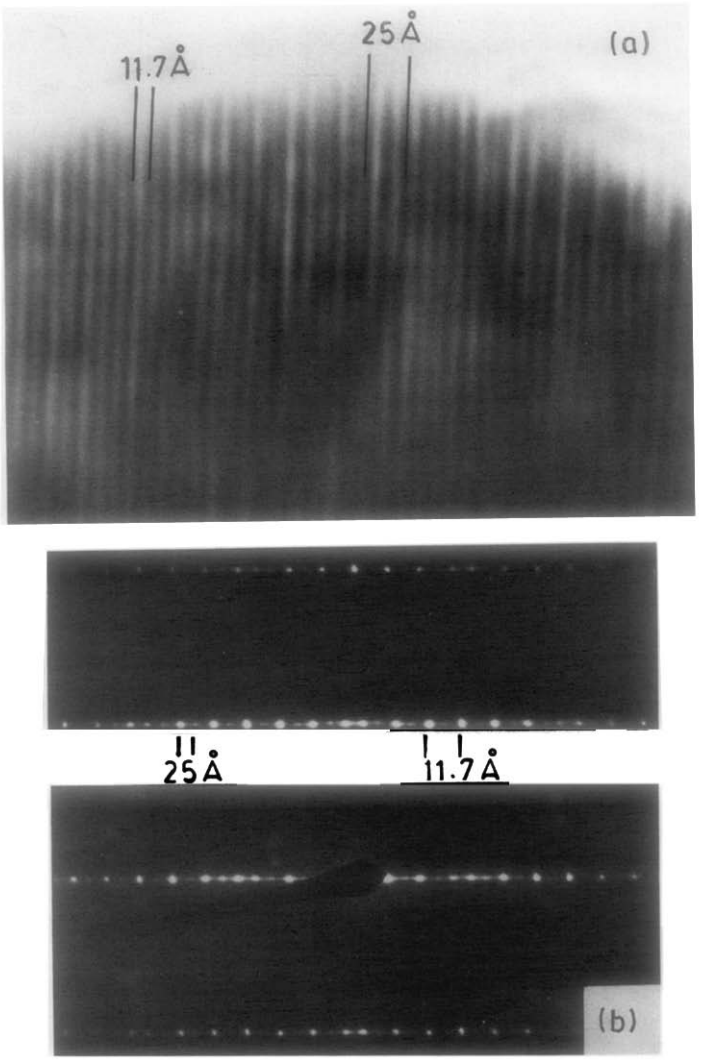

FIG. 15. (a) Lattice image showing intergrowth of 11.7 and 25 Å fringes corresponding to $YBa_2Cu_3O_7$ and $Y_2Ba_4Cu_7O_{15}$; (b) SAED pattern of (a) Bragg spots corresponding to 11.7 and 25 Å.

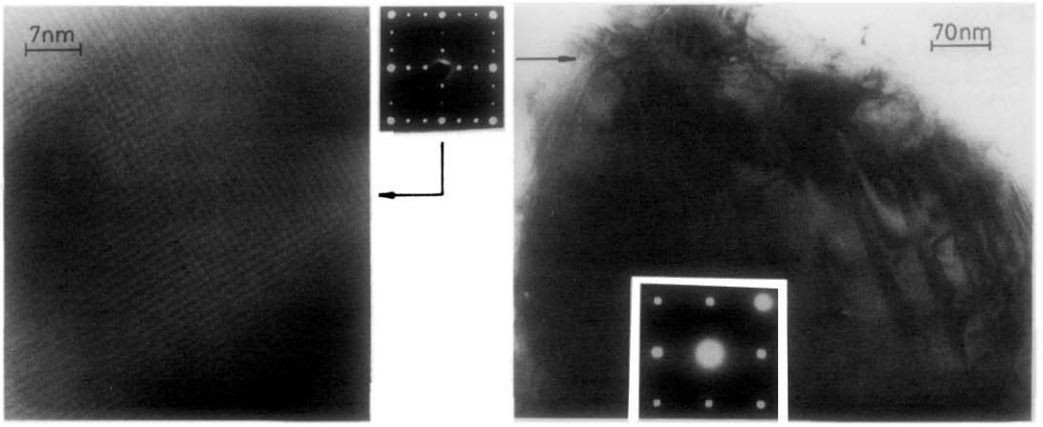

FIG. 16. Bright-field image (showing twins) and the lattice image corresponding to microdomains of $DyBa_2Cu_3O_7$ observed in a preparation of $Dy_2Ba_4Cu_7O_{15}$.

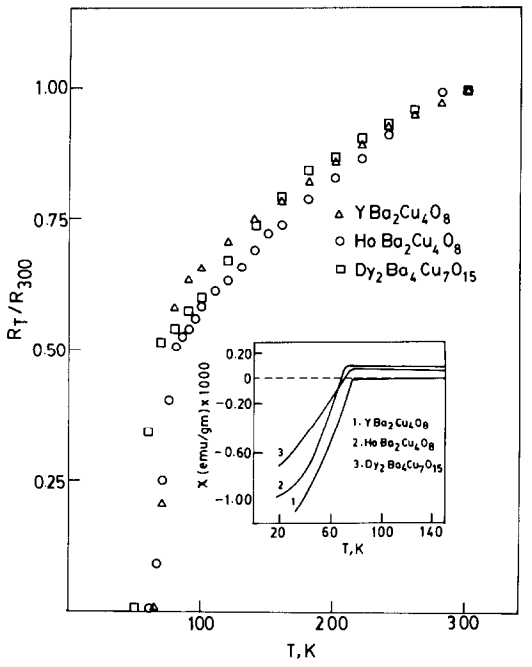

FIG. 17. Temperature variation of the normalized resistivity of 124 and 247 cuprates. Inset shows the DC magnetic susceptibility of a few members of 124 and 247 cuprates.

Acknowledgments

The authors thank the Department of Science and Technology, the Government of India, and the U.S. National Science Foundation for support of this research.

References

1. C. N. R. RAO, *Acc. Chem. Res.* **22,** 106 (1989); T. V. RAMAKRISHNAN AND C. N. R. RAO, *J. Phys. Chem.* **93,** 4414 (1989).
2. R. NAGARAJAN, R. VIJAYARAGHAVAN, L. GANAPATHI, R. A. MOHAN RAM, AND C. N. R. RAO, *Physica C* **158,** 453 (1989).
3. R. BEYERS, B. T. AHN, G. GORMAN, AND R. A. HUGGINS, *Nature (London)* **340,** 619 (1989).
4. A. G. KACHTURYAN, S. V. SEMENOVASTAYA, AND J. W. MORIS, JR., *Phys. Rev. B* **37,** 2243 (1987).
5. C. J. HOU, A. MANTHIRAM, L. RABENBERG, AND J. B. GOODENOUGH, *J. Mater. Res.* **5,** 9 (1990).
6. S. V. BHAT, P. GANGULY, T. V. RAMAKRISHNAN, AND C. N. R. RAO, *J. Phys. C: Solid State* **20,** L559 (1987).
7. J. KARPINSKI, E. KALDIS, E. JILEK, AND B. BUCHER, *Nature (London)* **336,** 660 (1988).
8. D. E. MORRIS, J. H. NICKEL, J. Y.T. WEI, N. G. ASMAR, J. S. SCOTT, U. M. SCHEVEN, C. T. HULTGREN, A. G. MARKELZ, J. E. POST, P. J. HEANEY, D. R. VEBLEN, AND E. M. HAZEN, *Phys. Rev. B* **39,** 7347 (1989); also *Phys. Rev. B* **40,** 11,406 (1989).
9. R. J. CAVA, J. J. KRAJEWSKI, W. F. PECK, JR., B. BATLOGG, L. W. RUPP JR., R. M. FLEMING, A. C. W. P. JAMES, AND P. MARSH, *Nature (London)* **338,** 328 (1989).
10. J. L. TALLON, D. M. POOKE, R. G. BUCKLEY, M. R. PRESLAND, AND F. J. BLUNT, *Phys. Rev. B* **41,** 7220 (1990).
11. M. A. ALARIO-FRANCO, C. CHAILLOUT, J. J. CAPPONI, J. CHENAVAS, AND M. MAREZIO, *Physica C* **156,** 455 (1988).
12. Y. HARIHARAN, A. BHARATHI, M. P. JANAWADKAR, D. VASUMATHI, V. S. SASTRY, AND T. S. RADHAKRISHNAN, *Physica C* **162–164,** 887 (1989).
13. J. GOPALAKRISHNAN, A. RAMANAN, C. N. R. RAO, D. A. JEFFERSON, AND D. J. SMITH, *J. Solid State Chem.* **55,** 101 (1984).
14. C. N. R. RAO AND J. M. THOMAS, *Acc. Chem. Res.* **18,** 113 (1985).
15. P. SOMASUNDARAM, R. A. MOHAN RAM, A. M. UMARJI, AND C. N. R. RAO, *Mater. Res. Bull.* **25,** 331 (1990).